CONSTRAINTS ON THE ORIGIN OF PHOBOS USING MAJOR ELEMENT DATA OBTAINED BY MMX MEGANE. K. Hirata[1,2], T. Usui[2], R. Hyodo[2], H. Genda[3], R. Fukai[2], D. J. Lawrence[4], N. L. Chabot[4], P. N. Peplowski[4]
[1]Univ. of Tokyo (hirata-kaori444@g.ecc.u-tokyo.ac.jp), Tokyo, Japan [2]Institute of Space and Astronautical Science, JAXA, [3]Earth-Life Science Institute, Tokyo Institute of Technology, [4]Johns Hopkins University Applied Physics Laboratory, Laurel, MD, USA.

Introduction: Phobos and Deimos are witness plates for the formation of the Mars-moon system. Two leading hypotheses for the origins of Phobos and Deimos have been proposed: the asteroid capture [1,2] and the giant impact [3,4] hypotheses. The circular and coplanar orbital properties of Phobos and Deimos favor the giant impact scenario, whereas their reflectance spectra, similar to D-type asteroids, support the capture origin. This controversy partly arises from the surface reflectance spectra that would have been modified by space weathering and late accretions [5–8]. Thus, this study focuses on the bulk elemental composition of Phobos to constrain Phobos' origin because the bulk composition represents the original building blocks, either a captured asteroid or a mixture of the impactor and the Martian crustal materials [9].

The Mars-moon Exploration with GAmma rays and NEutrons (MEGANE), which is a science payload of Martian Moons eXploration (MMX) mission, enables measurement of the bulk elemental abundances of Phobos using gamma-ray and neutron spectroscopy [10]. This study constructs a multivariate mixing model of Phobos' bulk elemental composition and examines the model's performance to discriminate the Phobos' origin hypotheses as a function of MEGANE's planned measurement capabilities.

Mixing model: Our mixing model assumes that Phobos consists of a mixture of materials from Mars and chondrite parent bodies [4] (Fig. 1); note that a captured scenario yields a zero Martian contribution. We employ a set of variables that consist of five elements (O, Mg, Si, Ca, and Fe) that would preserve the initial composition of the starting building blocks due to their lithophile and refractory characteristics. We assume 13 types of compositions from the 12 subgroups (CI, CM, CO, CV, CK, CR, H, L, LL, R, EH, and EL) of chondrites and ungrouped one (Tagish Lake) as end-components of the starting building blocks (a captured body or an impactor). Each starting composition has relative compositional variations of 10% for the five elements [11,12]. In our 5-component mixing model, Phobos' composition can be expressed as

$$P = MR \quad \text{(Eq. 1)}$$

where P = a Phobos composition measured by MEGANE, M = matrix of Mars and asteroid compositions. Then, the mixing ratio R is provided by

$$R = M^{-1}P \quad \text{(Eq. 2).}$$

The P includes a relative error (E_P) of 0, 10, and 20%. R ranges from 50% (the previous thermodynamical calculation the range of 30-70% [4]) in the impact scenario or 100 % in the asteroid capture scenario.

The 5-component mixing model determines if a measured Phobos composition (P) satisfies the mixing equation Eq. 1 for the four cases: (1) P constitutes a single end-component (i.e., the capture of an asteroid), (2) P represents a mixture of an end-component and the bulk-silicate Mars (BSM) (i.e., giant impact origin), (3) P returns non-unique R values (i.e., both the asteroid capture and the giant impact scenarios satisfy Eq.1 simultaneously), and (4) no variable sets of R and M satisfy Eq. 1 at any P (i.e,. no solution for Eq. 1). Thus, the Cases-1 and -2 yield a unique solution for Phobos' origin, whereas Cases-3 and -4 do not identify the origin. We conducted the mixing calculations for the 13 end-member compositions and determined the case at all P in the 5-element compositional spaces. The performance of our mixing model was evaluated by the discrimination performance D [%] at a measured Fe-Si composition,

$$D = \frac{[\text{Case}-1]+[\text{Case}-2]}{[\text{Case}-1]+[\text{Case}-2]+[\text{Case}-3]} \times 100 \quad \text{(Eq. 3).}$$

Effect of bulk compositions on the discrimination performance: First we considered the most simple case without any observation error (E_P = 0%). Our model indicates that MEGANE can uniquely determine the origin for >70% of the compositional space if E_P = 0 % (Fig. 2). For example, the origin of Phobos can be determined in the highest probability at P1 composition, 15 wt% Fe and 16 wt% Si (Fig. 2a). As there is no end-component composition overlapping P1, the capture origin should not fit (Case-2), resulting in 100% of D. We also show the most difficult example to determine the origin, the example at P2 composition, 23 wt% Fe and 19 wt% Si (Fig. 2b). Fe-Si composition at P2 can be explained either by some of the end-components (e.g., L, EL, R) or the mixing of BSM and other types of end-components (e.g., H, EH). Nevertheless, ~70% of the P space yield a unique origin (Cases-1 or -2). Next, we considered the case of E_P = 20% (Fig. 3). Mixing calculation indicates that the larger compositional spaces are classified as Case-3 and D decrease to 60% at P1 and 40% at P2.

Fig. 4 summarizes that the discrimination performance (D) depends on the measured Fe-Si composition of Phobos (P1 or P2). Again, the lower D at P2 than P1

in all range of E_P is attributable to the overlap of several types of chondrites around P2. This suggests that, if Phobos has a bulk composition similar to these types of chondrites (e.g., L, EL, R), these five major elements from the MEGANE data may not provide unique constraints on Phobos' origin without additional MEGANE element measurements, such as the trace elements U and Th or volatile elements K and Na, and the mineralogical and petrologic information obtained by other onboard instruments and the analyses of the returned sample [9].

Relationship between the MEGANE observation error and discrimination performance: Discrimination performance is also dependent on the MEGANE observation error (Fig. 4). The MEGANE instrument performance and initial MMX operations plan yielded estimated one-standard-deviation measurement uncertainties of ~20% for Fe and Si, and 33% for O, Mg, and Ca [10]. The relative precision of gamma-ray and neutron measurements is strongly dependent on the total acquired measurement time and the altitude of the measurements [13]. If the MMX mission is able to obtain MEGANE measurements beyond 10 days of accumulated time at altitudes lower than 1 body radius used to provide the current sensitivity estimates [10], then the relative precision of MEGANE's measurements can be improved. The inclusion of additional MEGANE measured elements beyond the five major elements included in this study will also improve the discrimination performance.

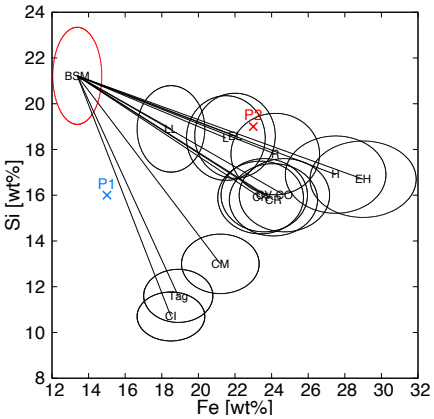

Fig. 1 The composition of bulk-silicate Mars (BSM, red circle) and 13 types of chondrites (black circles) in the Fe-Si diagram. The measured Phobos' composition would plot on a black circle for the capture origin (Case-1), or a solid black line for the impact origin (Case-2). P1 (Fe = 15 wt%, Si = 16 wt%) and P2 (Fe = 23 wt%, Si = 19 wt%) indicate data points shown in the Ca-Mg-O diagrams (Figs. 2 and 3).

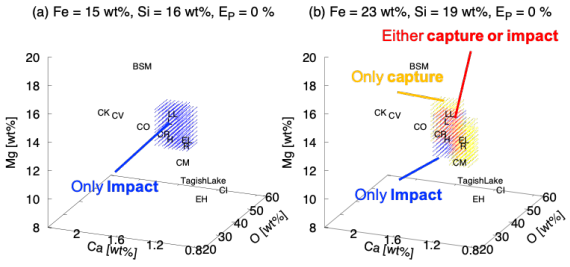

Fig. 2. The results of mixing calculations in the O-Ca-Mg diagrams for E_P = 0% at (a) P1 and (b) P2 in Fig. 1. Case-1: yellow, Case-2: blue, Case-3: red.

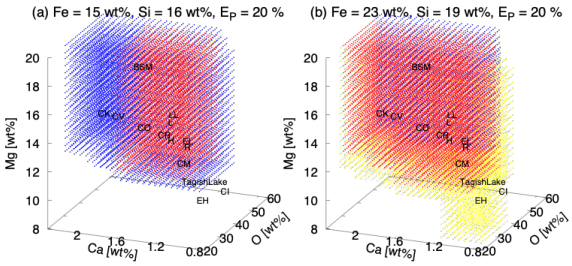

Fig. 3. The results of mixing calculations in the O-Ca-Mg diagrams for E_P = 20% at (a) P1 and (b) P2 in Fig. 1. Case-1: yellow, Case-2: blue, Case-3: red.

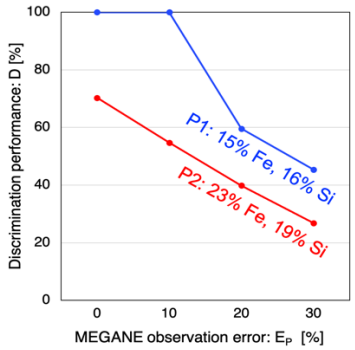

Fig. 4. Relationship between discrimination performance and MEGANE observation error (E_P = 0-30 %).

References: [1] Burns, J. A. (1992) *Mars,* 1283-1301. [2] Murchie, S. L. et al. (1991) *JGR*, *96*, 5925-5945. [3] Rosenblatt, P. et al. (2016) *Nature Geo. 9(8)*, 581-583. [4] Hyodo, R. et al. (2017) *Astrophys. J. 845*, 125. [5] Murchie, S. et al. (1999) *JGR, 104*, 9069-9079. [6] Rosenblatt, P. (2011) *Astron. Astrophys. Rev. 19*, 44. [7] Ramsley, K. R., & Head III, J. W. (2013) *Planet. Space Sci. 87*, 115-129. [8] Hyodo, R. et al. (2019) *Sci. Rep*. 9, 1-6. [9] Usui, T. et al. (2020) *Space Sci. Rev*, *216*, 49. [10] Lawrence, D. J. et al. (2019) *Earth Space Sci. 6*, 2605-2623. [11] Alexander, C. M. D. (2019a) *Geochim. Cosmochim. Acta*, *254*, 246-276. [12] Alexander, C. M. D. (2019b) *Geochim. Cosmochim. Acta*, *254*, 277-309. [13] Peplowski, P. N. (2016) *PSS 134*, 36-51.